Insights into Solid-State Electron Transport through Proteins from Inelastic Tunneling Spectroscopy: The Case of Azurin

Xi Yu,[†] Robert Lovrincic,[‡] Lior Sepunaru,[†] Wenjie Li,[†] Ayelet Vilan,[†] Israel Pecht,[*,§] Mordechai Sheves,[*,⊥] and David Cahen[*,†]

[†]Department of Materials and Interfaces, [§]Department of Immunology, and [⊥]Department of Organic Chemistry, Weizmann Institute of Science, Rehovot 76100, Israel and [‡]Institute for High Frequency Technology, TU Braunschweig, and Innovationlab, Speyerer Str. 4, 69115 Heidelberg, Germany

ABSTRACT Surprisingly efficient solid-state electron transport has recently been demonstrated through "dry" proteins (with only structural, tightly bound H_2O left), suggesting proteins as promising candidates for molecular (bio)electronics. Using inelastic electron tunneling spectroscopy (IETS), we explored electron−phonon interaction in metal/protein/metal junctions, to help understand solid-state electronic transport across the redox protein azurin. To that end an oriented azurin monolayer on Au is contacted by soft Au electrodes. Characteristic vibrational modes of amide and amino acid side groups as well as of the azurin−electrode contact were observed, revealing the azurin native conformation in the junction and the critical role of side groups in the charge transport. The lack of abrupt changes in the conductance and the line shape of IETS point to far off-resonance tunneling as the dominant transport mechanism across azurin, in line with previously reported (and herein confirmed) azurin junctions. The inelastic current and hence electron−phonon interaction appear to be rather weak and comparable in magnitude with the inelastic fraction of tunneling current *via* alkyl chains, which may reflect the known structural rigidity of azurin.

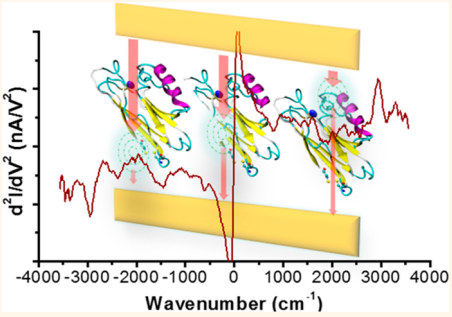

KEYWORDS: electron transfer · phonon-coupled electron transport · molecular electronics · inelastic electron tunneling spectroscopy

Electron transfer (ET) from donor to acceptor sites between and within proteins is central to biological energy conversion processes, from photosynthesis to respiration, and has been investigated extensively in solution, using techniques such as photolysis and electrochemistry.[1,2] For measurements of solid-state electron transport (ETp) *via* "dry" proteins (with only structural, tightly bound H_2O) in junctions, donor and acceptor are replaced by metallic electrodes and electron transport is measured as the voltage-dependent conductance (so-called $I-V$ characteristics). Its temperature dependence enables exploring the mechanism of the process, also *via* proteins, using the concepts and methods of solid-state physics. Recent work revealed surprisingly efficient electronic transport *via* proteins, suggesting them as potential candidates for biomolecular electronics.[3−6]

Over the past decade, molecular electronics[7−12] has witnessed significant progress from establishing experimental methods and investigating off-resonance tunneling electron transport to pursuing many-body phenomena such as electron−phonon or −photon interactions and their combination.[13−15] Of particular interest for the latter types of interactions are novel assembly units, where numerous intrinsic features of the molecules come into play. By considering such features we do not view molecules anymore acting "just" as dielectric barriers of a given (energy) height and (spatial) length for nonresonant tunneling transport. Proteins are interesting candidates as such assembly units, considering, for example, their chemical recognition properties and because some of them have electron transfer as their natural function. Long-range (single-step) tunneling, hopping ("multistep tunneling"), and combined multipathway electron

* Address correspondence to israel.pecht@weizmann.ac.il, mudi.sheves@weizmann.ac.il, david.cahen@weizmann.ac.il.

Received for review June 7, 2015 and accepted September 18, 2015.

Published online September 18, 2015
10.1021/acsnano.5b03950

transfer[16,17] have been invoked to explain the ET between and within proteins, depending on characteristics such as three-dimensional structure and their cofactor(s). However, combining the methods and experience of advanced solid-state with molecular electronics to the study of charge transport *via* proteins is only in its infancy.[5,6,18]

Exploring the interaction between transported electrons and molecular vibrations (phonons) is at the forefront of modern molecular electronics. It has been shown that electron−phonon interactions can strongly influence transport in simple organic molecule-based junctions.[13,19] Effects attributed to these interactions include phenomena such as coherent to incoherent transition with increasing electron/vibration interaction strength,[20,21] heating and heat conduction in molecular transport junctions,[22,23] and electronic current-induced chemical reactions.[24,25] Inelastic electron tunneling spectroscopy, IETS, has been used to provide insight into molecular electronics by helping the understanding of electron transport mechanisms and guiding the design of device structures, based on electron−phonon coupling.[13,19,26] It is not surprising that electron−phonon interactions also play a critical role in ET *via* proteins, especially in the long-range tunneling process between a donor and acceptor that are parts of, or bound to, a protein.[27,28]

The effect of electron−phonon interactions is twofold: First, vibrations can change the tunneling matrix element, which is a sensitive function of the protein's atomic configurations during the ET process. An example is the observation of weak electron−phonon coupling situations by IETS.[29−31] Second, vibrations can modulate interference between electrons in multipathway tunneling, to possibly trigger an otherwise forbidden kinetic process. This was demonstrated recently in model organic molecular junctions.[32]

Here we present the results of our investigation of phonon-coupled ETp in oriented protein monolayers that maintain their native conformation. We demonstrate the feasibility of resolving inelastic tunneling effects in current transport across protein-based junctions and use the results to identify the protein in the junction and to obtain insight into the ETp mechanism, which is fundamentally different from the well-studied ET process.[6]

IETS is an all-electronic spectroscopic method used to probe the interaction of electronic current with vibrational modes in molecules.[13,26] IETS of molecular junctions has been used primarily to confirm the actual presence of the molecules in the junction.[33,34] In some cases it has been argued that it can also provide information on the nature of the interfaces,[35,36] on the orientation of the molecules,[37] and even on the electron tunneling pathway.[38,39] Early IETS research included studies of biologically important molecules such as RNA and DNA[40] and even myoglobin by Hansma and co-workers.[13] In those early studies the (inorganic) insulator in metal−insulator−metal junctions was doped with the (bio)organic molecule of interest. IETS measurements on such samples provided information on the vibrational modes of the molecules involved. However, as the organic molecules were positioned in random orientations and with ill-defined coverage of these junctions, merely acting as dopant of the main (inorganic) tunneling barrier, no conclusions on the ETp properties of the molecules could be drawn.

We apply IETS to study the ETp across azurin (Az), a copper-containing protein that functions as an electron carrier in bacterial energy conversion systems. It has been studied extensively as a model of a redox-active protein with unique long-range ET properties by methods such as pulse radiolysis,[41,42] electrochemistry,[43,44] scanning probe methods (conducting probe AFM or (EC)STM),[45−47] and solid-state junctions.[3,48] By utilizing the redox property of the Cu ion, it was also used to build functional devices, such as transistors,[49] memory,[50] and a possible switch *via* negative differential resistance.[51]

To that end we prepared Az solid-state junctions that are stable and reproducible. We achieved this by forming an oriented Az monolayer on lithographically prepared microscopic Au electrodes and by using electrostatic trapped Au nanorods to form the junctions. The monolayer that we prepared (see experimental details) covers the substrate well so that one of the two Au/protein/Au formed junctions is not shorted (see also Results and Discussion); that is, any pinholes that are present after contact formation are too small to allow contact penetration.

We identified in the IET spectrum vibrational modes of Au−S, S−C, and amide, providing *prima facie* evidence that the examined junction contains amides and gold-bonded cysteine species, as expected for a solid-state protein junction. Compared to IR spectra of Az, we observe a relatively strong feature between the well-known amide I and II peaks. This pendant-group-related mode and the strong C−H stretching mode suggest that the transported charge interacts with the amino acids' side groups, in addition to the peptide amide. The line shape of the IETS implies far off-resonance tunneling as the dominant transport mechanism[39] across azurin and no electronic resonances up to ±0.5 V with molecular energy levels, which is surprising considering the presence of the Cu^{2+} metal ion. This finding suggests that the role of the redox-active centers in ETp process is fundamentally different from their redox activity in the ET process, as has been suggested earlier, based on results of temperature-dependent conductance measurements and optical spectroscopy.[3,6,48,52]

RESULTS AND DISCUSSION

In order to avoid damaging or denaturing the protein during monolayer junction formation, the protein

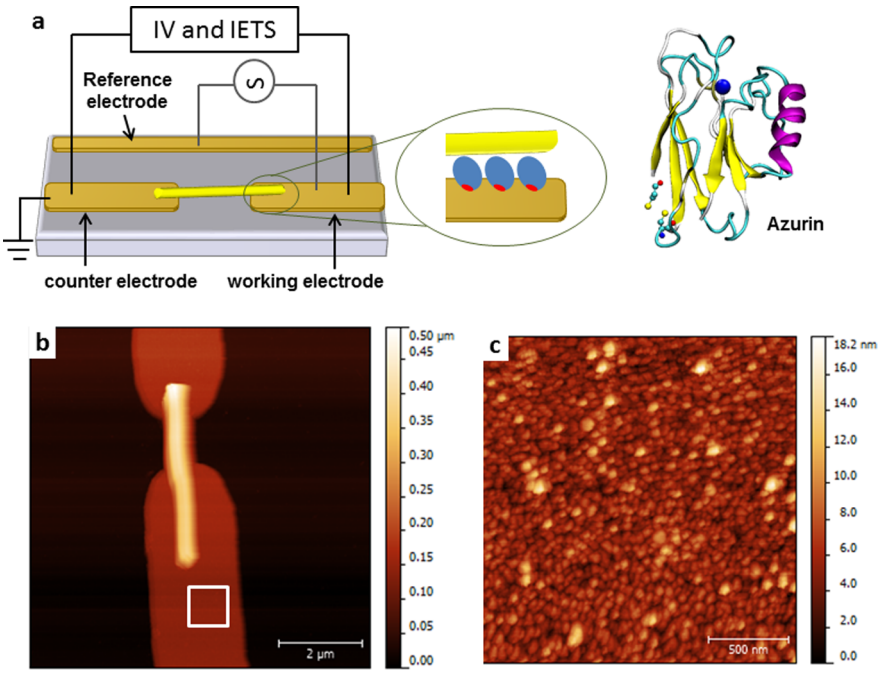

Figure 1. (a) Scheme of the Azurin junction fabricated by trapping nanowires by an ac electric field and *I*−*V* and IETS measurement. (b) Atomic force microscopic image of the nanowire, lying on the working and counter electrodes, after the electrostatic trapping. (c) AFM image of the square that is indicated in image (b), showing dense monolayer Az clusters on the gold electrode.

has to be contacted electrically in a "soft", nondestructive manner. Furthermore, the contact has to form a junction that is stable over a broad temperature range and allows low-noise current−voltage measurements for collection of meaningful IET spectra. To this end, we used the "suspended-wire" technique[53,54] to fabricate the solid-state Az junction. Basically a self-assembled monolayer of oriented Az was coupled covalently to a Au substrate by a S−Au bond between the Au and one of the relatively exposed Az cysteine thiolates. Au nanowires with a diameter of ~300 nm and length of ~4 μm were trapped onto the microelectrodes, using dielectrophoresis by applying an ac bias between working and reference electrodes (see Figure 1a and the Supporting Information) and using water as dielectric medium.[55] This is illustrated in Figure 1b, showing an AFM image of a nanowire, laid on the electrodes, forming a Au−protein−Au junction. The Az molecules form a dense, smooth array on the microelectrodes, as observed by AFM imaging (Figure 1c); its thickness, verified by both AFM and ellipsometry, confirms the presence of a monolayer of Az on the gold electrodes. Although one could expect two molecular (Au−protein−Au) junctions to be formed at each contact point of the nanowire with the Az-coated microelectrodes, it has been shown by Selzer and co-workers and confirmed by us, using CP-AFM (see Supporting Information), that only one junction is formed in this way, while the other contact presents a metal-to metal-short circuit.[56]

Temperature-dependent current−voltage (*I*−*V*) measurements were performed on the Au microelectrodes−Az−Au nanowire junctions by scanning between −1 and +1 V. As can be seen in Figure 2, the *I*−*V* pattern is quite symmetric around 0 V, indicating that the Au (substrate)−protein−Au (nanowire) junction has a symmetric potential profile, regardless of the different configuration of the Au electrodes (nanowire compared with evaporated) and the different binding strengths (chemisorption to microelectrode compared with van der Waals contact to the nanowire). Conduction *via* the junction was temperature-independent between 275 and 25 K, with only slight instabilities at some temperatures, probably due to small mechanical changes of the junction by mismatched thermal expansion and contraction. This is consistent with our previous results, obtained with Si−Az−Hg junctions and with Au substrate−Az−Au AFM tip junctions, using conducting probe AFM measurements, establishing that temperature-independent conduction is intrinsic for holo-Az. The good correlation between *I*−*V* curves of Az measured *via* the suspended wire junctions and those *via* former junction configurations confirms the reliability of suspended wires for measuring protein monolayers.

The fact that the conductivity of Az does not decrease with temperature also helps to have a sufficient S/N ratio for the (low-temperature) IETS measurements. Considering the low currents through small contact area junctions, Az provides significantly higher currents at low temperatures than can be obtained *via*

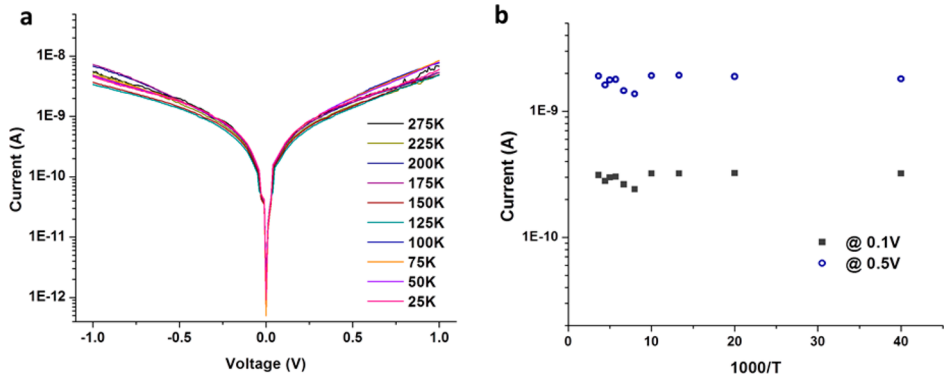

Figure 2. Temperature-dependent voltage−current curves *via* the Azurin junction: (a) full *I*−*V* characteristics between −1 and +1 V, with current plotted as log(*I*), at different temperatures and (b) current at +0.1 and +0.5 V, indicating a uniform behavior at different bias voltages (cf. ref 52).

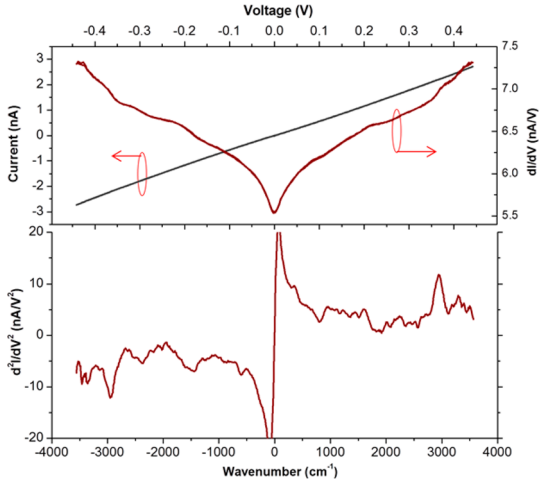

Figure 3. (Top) Current−voltage (black) and conductance−voltage (red) plots of the Az junction between −0.5 and +0.5 V. (Bottom) IET spectrum for the same junction. IETS is shown as d^2I/dV^2.

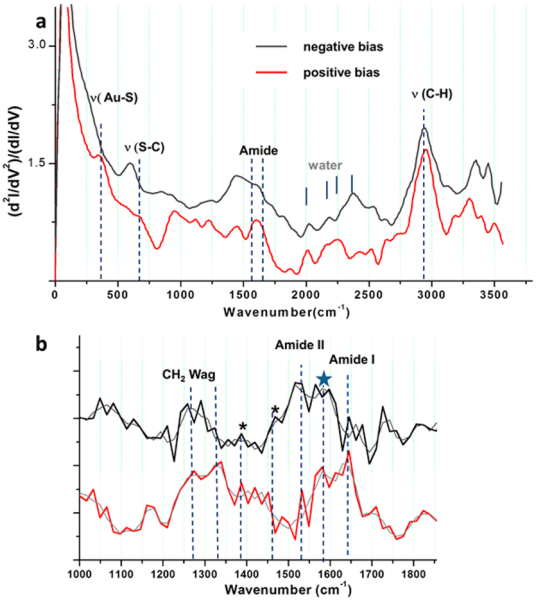

Figure 4. (a) IET spectrum of an Az junction. The gray and red lines are the spectra at negative and positive bias, respectively. (b) Higher resolution IET spectrum at around 5.5 K with an ac modulation amplitude of 6 mV. Tentative assignments of the peaks are based on previously reported IR spectra of the protein. Note the IETS (d^2I/dV^2) was normalized with d*I*/d*V* in order to correct the baseline in conductance.

most other proteins that we have studied, which exhibited significant thermally activated conduction down to 150−200 K and much lower conduction at 10 K than Az.[6]

For IETS measurements, first and second derivatives are recorded as the first and second harmonic signals, respectively, using lock-in techniques with a dc bias added to an ac signal at a frequency of 443 Hz and applied to the samples. Typical *I*−*V* and conductance (*G*)−V plots and IET spectra of azurin are shown in Figure 3, measured at around 10 K with an ac modulation amplitude of 8 mV. The nearly linear *I*−*V* curve (up to 0.5 V bias) and slight increase of *G* at higher bias are characteristic for off-resonance tunneling.[57] The step-like increase of *G* at certain voltages corresponds to peaks in the inelastic signal, and the dip near zero bias is the low bias anomaly usually attributed to the large number of low-energy vibrations including gold phonons.[38] The IET spectrum is quite symmetric, consistent with the symmetric *I*−*V* plot. The most significant and well-resolved peak in the IET spectrum is the C−H stretching peak at around 2900 cm^{-1}. This is similar to alkane molecular junctions, despite the much smaller fraction of C−H units in a protein. This result provides an important confirmation for a single junction and an accurate read of the vibration energy; in a scenario of a double Az junction between the two bottom electrodes and the bridging Au rod, the applied voltage would be divided and cause the C−H stretching peak to appear at a higher applied voltage, up to twice the vibration energy for an equipartition.

Closer illustration of the full IET spectrum and a higher resolution scan of part of the spectrum at lower temperature with smaller ac modulation (6 mV) are shown in Figure 4 and summarized in Table 1. It can be seen that the relative peak intensities and resultant IETS shapes are slightly different for positive and

TABLE 1. IETS Peaks and Mode Assignment

	peak position		
mode	mV	cm^{-1}	refs
ν(Au—S)	41	330 ± 10	60, 61 (IETS)
ν(S—C)	80, 87	650, 700 ± 10	30 (IETS and Raman)
CH_2 wag	160	~1300 ± 20	30 (IETS and IR)
amide II	188	1520 ± 8	62, 63 (IR)
conjugate or N—H wag?	196	1590 ± 10	62, 63 (IR)
amide I	203	1640 ± 8	62—64 (IR)
ν(C—H)	361	2910 ± 20	30 (IETS and IR)

negative bias, probably because of the asymmetric protein electrode contacts, with Au—S bonding of the protein to the bottom electrode and mechanical contact of the Au nanowire to the top end of the Az, proximal to the Cu binding site. Still, the main features are quite similar. Characteristic vibrational modes of the Au-bound Az can be identified on the basis of IR spectra of Az and on IETS studies of organic thiol monolayers. For example, the shoulder around 650 cm^{-1} (and 700 cm^{-1} peak, see Supporting Information Figure S4 and S5) can be assigned to C—S stretching[30] and the peak at around 330 cm^{-1} can be assigned as a Au—S stretching mode.[58—60] We ascribe these to the bond between one of the cysteine thiolates of Az and the gold electrodes. The intensity of these S-related modes is much stronger than the fraction of S in Az and suggests considerable scattering and resulting inelastic effects at the molecule/solid interface. This result further confirms the bonding of azurin on gold through one of the sulfides of the natural disulfide of cysteine on the surface of azurin and excludes the possibility of Az binding *via* Au—N bonds of exposed lysine residues, since no Au—N IETS signal (~240 cm^{-1})[61] was observed.

The IR of proteins is often studied as an indicator for their secondary structure, especially the amide I and amide II bands, due to the C═O stretching and the out-of-phase combination of NH bending and CN stretching, respectively.[62,63] We can tentatively assign the amide I and II modes in the IET spectra. These peaks at around 1640 and 1520 cm^{-1} are quite reproducible despite variation in their intensity under the two bias polarities. These characteristic modes provide direct evidence for the protein's presence between the electrodes and that the observed ETp properties indeed originate from the protein itself, rather than from impurities or condensed water molecules at low temperature. The position and shape of the amide I peak in the high-resolution IR spectrum of proteins have been used widely to reflect the secondary structure of proteins. Although the shape of the amide I peak is hard to resolve because of temperature and *ac* modulation broadening, the position of this peak is consistent with the reported IR results for Az in solution.[64] This indicates that Az maintains its native conformation in the solid-state junction, in agreement with our earlier conclusions, based on optical absorbance and fluorescence spectra and on the irreversible drop in current observed upon increasing the temperature of the ETp measurement to that of the protein's denaturation.[3,48]

The ~1600 cm^{-1} peak observed between the amide I and II ones with comparable amplitude is always present in the IET spectrum of Az, which is quite different from what is seen in the protein's IR spectrum, where the amide I and II peaks dominate. According to its frequency, this peak can be assigned to modes of the side groups of amino acids, such as the NH_2 in-plane bending (scissoring) and C═C or CN bond in conjugated side groups present in tyrosine, phenylalanine, and tryptophan.[62] Considering that IETS selects vibrations that are related to the electron transport pathway,[38] our results indicate that the side groups of the amino acids play a significant role in electron transport across proteins.[65] Clearer identification of the peaks by deuteration and by use of site-specific mutations, where groups like C═C or C═N can be replaced, should provide more insight into the role of the amino acid side groups.

The fingerprint band below 1500 cm^{-1} is generally very hard to identify and rarely used as such in the interpretation of the IR spectra of proteins; CH_2 wagging might be the only recognizable mode in this region. We note several features between the amide and C—H stretching peaks. In the range between 1900 and 2800 cm^{-1} there are few characteristic peaks except for the stretching mode of the carbon—carbon triple bond or a single bond such as S—H.[62] The IETS of the Az junction always showed some broad and low-intensity signal in this range. Since there is no triple bond in the bound Az, these peaks might be due to an S—H bond (if part of the natural disulfide group, after S—S cleavage, is not bound to the surface), and/or to residual water.[66]

An interesting outcome of the IETS of Az is what is missing in it. Electron—phonon interactions in molecular junctions can actually generate a variety of current—voltage characteristics. In general, experimental observations of inelastic electron tunneling can be classified according to whether electronic resonance is involved in the inelastic tunneling process or not. It has been found in theory and observed experimentally[67] that clear inelastic features appear as peaks in the far off-resonant regime with weak electron—phonon interaction, while if a resonance or near-resonance electronic state is involved, dips or derivative-like features may show up, because of strong electron—phonon interaction (polarization). Either this interaction will blur the IETS features, making characterization of the junction impossible, or, in some well-controlled situations, the position of the derivative-like features can be used to identify the corresponding chemical bonds that are involved in the polarization.[39]

It is indeed surprising to observe that transport *via* Az, which has a metal redox active site and a hierarchical structure, exhibits inelastic effects that are similar to those shown for transport across alkane organic molecules without a strong polarization effect[13] which is seen in molecular junctions with metal ions or metal nanoparticles[68,69] by virtue of their electronic states near the electrode Fermi level. We note, though, that our finding that ETp *via* Az is temperature-independent down to 10 K, is consistent with charge transport *via* tunneling. While there are other possible mechanisms that will yield temperature-independent transport,[70−72] the line shapes of the present IET spectra are consistent with off-resonance tunneling,[39,67] a conclusion that is consistent with that of Davis *et al*., where the *I*−*V* curves of the azurin monolayer, measured by conducting AFM, were found to fit Simon's model.[45,73]

In the far from resonance situation, where the energy gap between the molecular frontier orbitals (highest occupied system orbital (HOSO) or lowest unoccupied system orbital (LUSO)) and the nearest electrode Fermi energy level is large relative to the relevant phonon frequencies and corresponding electron−phonon couplings, this coupling leads to changes of the peak line shapes in IETS, *i.e*., conductance increase at the threshold energy of a certain vibrational mode. The inelastic contribution to the total current is around 2−3%, as deduced from the *G*−*V* data, comparable in magnitude to that found for alkyl chains.[31] Thus, despite the long-distance transport *via* Az, interactions of the transiting electrons with the Az polypeptide matrix and its bound (Cu) metal ion are apparently rather weak. This observation, which might be directly correlated with the above-mentioned efficient electron transport, may be a result of the known structural rigidity of azurin.

Consistent with the off-resonance tunneling mechanism, modes that are related to the ligands of Cu in its Az coordination site, *i.e*., Cu−N (histidine), Cu−O (glycine), and Cu−S (cysteine and methionine), which have been identified by resonance Raman spectra around 400 cm^{-1},[74,75] does not present as detectable signal in the IETS, although those modes have been suggested to be important for ET dynamics in azurin.[76,77]

We emphasize that our present findings do not exclude the participation of the Cu ion in the charge transport across azurin junctions. Our IETS line shape analysis can exclude only Cu-assisted resonance tunneling and hopping mechanisms and supports the off-resonance tunneling mechanism. Actually, this is a further indication for what was discussed and shown by us earlier, that solid-state charge transport (ETp) is fundamentally different from the electron transfer in biological systems,[3,5,6] as in the latter for Az, the $Cu^{2+} \longleftrightarrow Cu^{+}$ redox process is well known as the heart of the ET process. Research by Artés *et al*.[78,79] and Chi *et al*.[46] using electrochemical scanning tunneling microscopy (ECSTM) with electrochemical gating on single azurin has illustrated the Cu ion redox process in the charge transport at room temperature in a buffered environment. However, in contrast to what is the case for electrochemical measurements with the redox protein adsorbed on the electrode, in ETp of redox-active proteins measured *via* solid-state junctions, normally no redox process will be involved, as shown by us for Az[52] and Cyt C.[80] This is due to factors such as solvent environment, including mobile ions in solution, and the continuum of states of the electrodes, including coupling of the protein to the electrodes.[81,82] IETS experiments using azurin with different metal ions replacing the Cu and gating experiments to tune the energy levels of the metal may be able to reveal more information on the role of the metal in the transport process.

CONCLUSION

In conclusion, we presented here results of the first study on phonon-coupled ETp across a well-defined and oriented metal−protein−metal solid-state-like junction, using inelastic tunneling spectroscopy. Characteristic vibrational modes such as the Au−S, S−C, C−H, amide I and amide II, as well as some that can be assigned to amino acid side groups, were observed, which clearly show that inelastic transport occurs through the protein. Remarkably, the position of the C═O amide I mode was found to be the same as those of native azurin in solution, providing sound proof of the observed charge transport across the native protein in these solid-state junctions. Meanwhile, the mode at around 1600 cm^{-1} reveals the importance of the amino acid side groups in charge transport. The lack of dips or derivative peak shapes in the IETS of the Az junction provides evidence for the absence of electronic interactions with the molecular levels, despite the presence of Cu^{2+} with electronic states near the Fermi level of the gold electrode.[83] IETS is thus shown to be a powerful tool for investigating the ETp process in a protein-based junction. Studies of various Az derivatives and gated IETS are under way in our lab to further resolve the transport mechanism.

METHODS

Sample Preparation. The gold microelectrode substrate was fabricated on a Si-SiO_2 wafer by a standard microfabrication technique with sequential processes of photolithography, metal evaporation, and lift-off. Az monolayers were fabricated by placing a drop of Az solution (0.5 mg/mL, acetate buffer pH 4.8) on the substrate, which was cleaned and activated by UV ozone and hot ethanol, and incubated for 2 h at room temperature. Au nanowires were trapped onto the microelectrodes

by ac dielectrophoresis (details can be found in ref 56), using water as dielectric medium and a voltage of 3 V with 1 MHz frequency for 15 min.

Transport Measurement. Transport measurements were done in a Lakeshore TTPX cryogenic probe station using liquid helium and a temperature controller for cooling and adjusting the temperature. Conductance was measured with a subfemtoamp source-meter (Keithley 6430) operating with an automatic variable gain preamplifier. IET spectra were measured with a home-built system, which allows simultaneous measurement of differential conductance (dI/dV) and its derivative (d^2I/dV^2) (IETS) as first- and second-harmonic signals, using two lock-in amplifiers (Stanford Research Systems SR830). A dc bias added to an ac modulation of 8 or 6 mV at a frequency of 443 Hz was applied to the sample. All instruments, measurements with them, and data collection were controlled by a Labview program.

The IETS measurement was conducted generally at around 10 K with an ac modulation of 8 mV and a dc voltage step of 4 mV. For higher resolution, the measurement was conducted at around 5.5 K with an ac modulation of 6 mV and a dc step of 2 mV. To obtain a smooth spectroscopy line, a time constant of 100−300 ms for the lock-in amplifier was used, and 5 measurements for each bias value, at least 20 back and forth scans to average, were carried out. This procedure generally takes several hours. To further improve the validity of the results, we performed ≥5 independent measurements for >10 junctions. The signal-to-noise ratio arising from the IET spectra of the azurin samples was in general up to ∼6 dB.

Conflict of Interest: The authors declare no competing financial interest.

Acknowledgment. We thank Prof. Y. Selzer and R. Arielly (Tel Aviv University) for their kind help and guidance in preparing and trapping suspended Au nanowires for mesoscopic electrical contacts to soft matter. X.Y. thanks the Council for Higher Education (Israel) for a PBC program postdoctoral research fellowship. R.L. acknowledges a Minerva Foundation and subsequent Marie Curie IE Fellowship (FP7-PEOPLE-2011-IEF no. 29866), both held at the Weizmann Institute. L.S. thanks the Israel Ministry of Science for an Eshkol doctoral fellowship. We thank the Minerva Foundation (Munich), the Israel Science Foundation Centre of Excellence program, the Grand Centre for Sensors and Security, the Benoziyo Endowment Fund for the Advancement of Science, and the J & R Center for Scientific Research for partial support. M.S. holds the Ephraim Katzir/Rao Makineni Professorial Chair of Chemistry. D.C. holds the Sylvia and Rowland Schaefer Chair in Energy Research.

Supporting Information Available: The Supporting Information is available free of charge on the ACS Publications website at DOI: 10.1021/acsnano.5b03950.

Additional figures (PDF)

REFERENCES AND NOTES

1. Winkler, J.; Gray, H. Electron Flow through Metalloproteins. *Chem. Rev.* **2014**, *114*, 3369–3380.
2. Winkler, J.; Gray, H. Long-Range Electron Tunneling. *J. Am. Chem. Soc.* **2014**, *136*, 2930–29399.
3. Ron, I.; Sepunaru, L.; Itzhakov, S.; Belenkova, T.; Friedman, N.; Pecht, I.; Sheves, M.; Cahen, D. Proteins as Electronic Materials: Electron Transport through Solid-State Protein Monolayer Junctions. *J. Am. Chem. Soc.* **2010**, *132*, 4131–4140.
4. Jin, Y.; Honig, T.; Ron, I.; Friedman, N.; Sheves, M.; Cahen, D. Bacteriorhodopsin as an Electronic Conduction Medium for Biomolecular Electronics. *Chem. Soc. Rev.* **2008**, *37*, 2422–2432.
5. Ron, I.; Pecht, I.; Sheves, M.; Cahen, D. Proteins as Solid-State Electronic Conductors. *Acc. Chem. Res.* **2010**, *43*, 945–953.
6. Amdursky, N.; Marchak, D.; Sepunaru, L.; Pecht, I.; Sheves, M.; Cahen, D. Electronic Transport *via* Proteins. *Adv. Mater.* **2014**, *26*, 7142–7161.
7. Song, H.; Reed, M.; Lee, T. Single Molecule Electronic Devices. *Adv. Mater.* **2011**, *23*, 1583–1608.
8. Nitzan, A.; Ratner, M. A. Electron Transport in Molecular Wire Junctions. *Science* **2003**, *300*, 1384–1389.
9. Tao, N. J. Electron transport in molecular junctions. *Nat. Nanotechnol.* **2006**, *1*, 173–181.
10. Heath, J. Molecular Electronics. *Annu. Rev. Mater. Res.* **2009**, *39*, 1–23.
11. McCreery, R.; Bergren, A. Progress with Molecular Electronic Junctions: Meeting Experimental Challenges in Design and Fabrication. *Adv. Mater.* **2009**, *21*, 4303–4322.
12. Ratner, M. A Brief History of Molecular Electronics. *Nat. Nanotechnol.* **2013**, *8*, 378–381.
13. Galperin, M.; Ratner, M.; Nitzan, A.; Troisi, A. Nuclear Coupling and Polarization in Molecular Transport Junctions: Beyond Tunneling to Function. *Science* **2008**, *319*, 1056–1060.
14. Galperin, M.; Nitzan, A. Molecular Optoelectronics: The Interaction of Molecular Conduction Junctions with Light. *Phys. Chem. Chem. Phys.* **2012**, *14*, 9421–9438.
15. Bergfield, J.; Ratner, M. Forty Years of Molecular Electronics: Non-Equilibrium Heat and Charge Transport at the Nanoscale. *Phys. Status Solidi B* **2013**, *250*, 2249–2266.
16. Skourtis, S. Probing Protein Electron Transfer Mechanisms from the Molecular to the Cellular Length Scales. *Biopolymers* **2013**, *100*, 82–92.
17. Beratan, D.; Skourtis, S.; Balabin, I.; Balaeff, A.; Keinan, S.; Venkatramani, R.; Xiao, D. Steering Electrons on Moving Pathways. *Acc. Chem. Res.* **2009**, *42*, 1669–1678.
18. Shinwari, M.; Deen, M.; Starikov, E.; Cuniberti, G. Electrical Conductance in Biological Molecules. *Adv. Funct. Mater.* **2010**, *20*, 1865–1883.
19. Galperin, M.; Ratner, M. A.; Nitzan, A. Molecular transport junctions: vibrational effects. *J. Phys.: Condens. Matter* **2007**, *19*, 103201.
20. Galperin, M.; Ratner, M.; Nitzan, A. Hysteresis, Switching, and Negative Differential Resistance in Molecular Junctions: A Polaron Model. *Nano Lett.* **2005**, *5*, 125–130.
21. Kubatkin, S.; Danilov, A.; Hjort, M.; Cornil, J.; Brédas, J.-L.; Stuhr-Hansen, N.; Hedegård, P.; Bjørnholm, T. Single-Electron Transistor of a Single Organic Molecule with Access to Several Redox States. *Nature* **2003**, *425*, 698–701.
22. Frederiksen, T.; Brandbyge, M.; Lorente, N.; Jauho, A.-P. Inelastic Scattering and Local Heating in Atomic Gold Wires. *Phys. Rev. Lett.* **2004**, *93*, 256601.
23. Chen, Y.-C.; Zwolak, M.; Di Ventra, M. Local Heating in Nanoscale Conductors. *Nano Lett.* **2003**, *3*, 1691–1694.
24. Pascual, J. Single Molecule Vibrationally Mediated Chemistry. *Eur. Phys. J. D* **2005**, *35*, 327–340.
25. Seideman, T. Current-Driven Dynamics in Molecular-Scale Devices. *J. Phys.: Condens. Matter* **2003**, *15*, R521–R549.
26. Hihath, J.; Tao, N. Electron−phonon Interactions in Atomic and Molecular Devices. *Prog. Surf. Sci.* **2012**, *87*, 189–292.
27. Medvedev, E.; Stuchebrukhov, A. Inelastic Tunneling in Long-Distance Biological Electron Transfer Reactions. *J. Chem. Phys.* **1997**, *107*, 3821–3831.
28. Daizadeh, I.; Medvedev, E.; Stuchebrukhov, A. Effect of Protein Dynamics on Biological Electron Transfer. *Proc. Natl. Acad. Sci. U. S. A.* **1997**, *94*, 3703–3708.
29. Kushmerick, J.; Lazorcik, J.; Patterson, C.; Shashidhar, R.; Seferos, D.; Bazan, G. Vibronic Contributions to Charge Transport Across Molecular Junctions. *Nano Lett.* **2004**, *4*, 639–642.
30. Wang, W.; Lee, T.; Kretzschmar, I.; Reed, M. Inelastic Electron Tunneling Spectroscopy of an Alkanedithiol Self-Assembled Monolayer. *Nano Lett.* **2004**, *4*, 643–646.
31. Okabayashi, N.; Paulsson, M.; Komeda, T. Inelastic Electron Tunneling Process for Alkanethiol Self-Assembled Monolayers. *Prog. Surf. Sci.* **2013**, *88*, 1–38.
32. Ballmann, S.; Härtle, R.; Coto, P.; Elbing, M.; Mayor, M.; Bryce, M.; Thoss, M.; Weber, H. Experimental Evidence for Quantum Interference and Vibrationally Induced Decoherence in Single-Molecule Junctions. *Phys. Rev. Lett.* **2012**, *109*, 056801.

33. Simonsen, M. G.; Coleman, R. V.; Hansma, P. K. High Resolution Inelastic Tunneling Spectroscopy of Macromolecules and Adsorbed Species with Liquid Phase Doping. *J. Chem. Phys.* **1974**, *61*, 3789–3799.
34. Hipps, K. W.; Mazur, U. Inelastic Electron Tunneling: An Alternative Molecular Spectroscopy. *J. Phys. Chem.* **1993**, *97*, 7803–7814.
35. Kula, M.; Jiang, J.; Luo, Y. Probing Molecule-Metal Bonding in Molecular Junctions by Inelastic Electron Tunneling Spectroscopy. *Nano Lett.* **2006**, *6*, 1693–1698.
36. Long, D.; Lazorcik, J.; Mantooth, B.; Moore, M.; Ratner, M.; Troisi, A.; Yao, Y.; Ciszek, J.; Tour, J.; Shashidhar, R. Effects of Hydration on Molecular Junction Transport. *Nat. Mater.* **2006**, *5*, 901–908.
37. Lin, L. L.; Wang, C. K.; Luo, Y. Inelastic Electron Tunneling Spectroscopy of Gold− Benzenedithiol− Gold Junctions: Accurate Determination of Molecular Conformation. *ACS Nano* **2011**, *5*, 2257–2263.
38. Troisi, A.; Beebe, J.; Picraux, L.; van Zee, R.; Stewart, D.; Ratner, M.; Kushmerick, J. Tracing Electronic Pathways in Molecules by Using Inelastic Tunneling Spectroscopy. *Proc. Natl. Acad. Sci. U. S. A.* **2007**, *104*, 14255–14259.
39. Song, H.; Kim, Y.; Jang, Y.; Jeong, H.; Reed, M.; Lee, T. Observation of Molecular Orbital Gating. *Nature* **2009**, *462*, 1039–1043.
40. Hansma, P.; Coleman, R. Spectroscopy of Biological Compounds with Inelastic Electron Tunneling. *Science* **1974**, *184*, 1369–1371.
41. Wherland, S.; Farver, O.; Pecht, I. Multicopper Oxidases: Intramolecular Electron Transfer and O2 Reduction. *JBIC, J. Biol. Inorg. Chem.* **2014**, *19*, 541–554.
42. Farver, O.; Pecht, I. Blue Copper Proteins as a Model for Investigating Electron Transfer Processes within Polypeptide Matrices. *Biophys. Chem.* **1994**, *50*, 203–216.
43. Chi, Q.; Zhang, J.; Nielsen, J.; Friis, E.; Chorkendorff, I.; Canters, G.; Andersen, J.; Ulstrup, J. Molecular Monolayers and Interfacial Electron Transfer of Pseudomonas aeruginosa Azurin on Au(111). *J. Am. Chem. Soc.* **2000**, *122*, 4047–4055.
44. Khoshtariya, D.; Dolidze, T.; Shushanyan, M.; Davis, K.; Waldeck, D.; van Eldik, R. Fundamental Signatures of Short- and Long-Range Electron Transfer for the Blue Copper Protein Azurin at Au/SAM Junctions. *Proc. Natl. Acad. Sci. U. S. A.* **2010**, *107*, 2757–2762.
45. Zhao, J.; Davis, J. J.; Sansom, M. S.; Hung, A. Exploring the Electronic and Mechanical Properties of Protein Using Conducting Atomic Force Microscopy. *J. Am. Chem. Soc.* **2004**, *126*, 5601–5609.
46. Chi, Q.; Farver, O.; Ulstrup, J. Long-Range Protein Electron Transfer Observed at the Single-Molecule Level: *In Situ* Mapping of Redox-Gated Tunneling Resonance. *Proc. Natl. Acad. Sci. U. S. A.* **2005**, *102*, 16203–1608.
47. Li, W.; Sepunaru, L.; Amdursky, N.; Cohen, S.; Pecht, I.; Sheves, M.; Cahen, D. Temperature and Force Dependence of Nanoscale Electron Transport *via* the Cu Protein Azurin. *ACS Nano* **2012**, *6*, 10816–10824.
48. Sepunaru, L.; Pecht, I.; Sheves, M.; Cahen, D. Solid-State Electron Transport across Azurin: From a Temperature-Independent to a Temperature-Activated Mechanism. *J. Am. Chem. Soc.* **2011**, *133*, 2421–2423.
49. Artés, J.; Díez-Pérez, I.; Gorostiza, P. Transistor-like Behavior of Single Metalloprotein Junctions. *Nano Lett.* **2012**, *12*, 2679–2684.
50. Lee, T.; Kim, S.; Min, J.; Choi, J. Multilevel Biomemory Device Consisting of Recombinant Azurin/Cytochrome c. *Adv. Mater.* **2010**, *22*, 510–514.
51. Maruccio, G.; Marzo, P.; Krahne, R.; Passaseo, A.; Cingolani, R.; Rinaldi, R. Protein Conduction and Negative Differential Resistance in Large-Scale Nanojunction Arrays. *Small* **2007**, *3*, 1184–1188.
52. Amdursky, N.; Sepunaru, L.; Raichlin, S.; Pecht, I.; Sheves, M.; Cahen, D. Electron Transfer Proteins as Electronic Conductors: Significance of the Metal and Its Binding Site in the Blue Cu Protein, Azurin. *Adv. Sci.* **2015**, *2*, 1400026.
53. Smith, P.; Nordquist, C.; Jackson, T.; Mayer, T.; Martin, B.; Mbindyo, J.; Mallouk, T. Electric-Field Assisted Assembly and Alignment of Metallic Nanowires. *Appl. Phys. Lett.* **2000**, *77*, 1399–1401.
54. Freer, E.; Grachev, O.; Duan, X.; Martin, S.; Stumbo, D. High-Yield Self-Limiting Single-Nanowire Assembly with Dielectrophoresis. *Nat. Nanotechnol.* **2010**, *5*, 525–530.
55. Smith, B.; Mayer, T.; Keating, C. Deterministic Assembly of Functional Nanostructures Using Nonuniform Electric Fields. *Annu. Rev. Phys. Chem.* **2012**, *63*, 241–263.
56. Noy, G.; Ophir, A.; Selzer, Y. Response of Molecular Junctions to Surface Plasmon Polaritons. *Angew. Chem., Int. Ed.* **2010**, *49*, 5734–5736.
57. Cuevas, J. C.; Scheer, E. *Molecular Electronics: An Introduction to Theory and Experiment*, 1st ed.; World Scientific Publishing Company, 2010.
58. The Au−S stretching mode is generally reported at around 290 cm^{-1} for alkane thiol monolayers. However, a mode at higher wavenumber, around 350 cm^{-1}, was also observed experimentally and in *ab initio* simulations. The differences are likely due to the details of the bonding, affecting the coupling strength of the S with the Au lattice or possible involvement of other vibrations coupled to the Au−S one (see refs 38, 60, and 61).
59. Hihath, J.; Bruot, C.; Tao, N. Electron−Phonon Interactions in Single Octanedithiol Molecular Junctions. *ACS Nano* **2010**, *4*, 3823–3830.
60. Arroyo, C.; Frederiksen, T.; Rubio-Bollinger, G.; Vélez, M.; Arnau, A.; Sánchez-Portal, D.; Agraït, N. Characterization of Single-Molecule Pentanedithiol Junctions by Inelastic Electron Tunneling Spectroscopy and First-Principles Calculations. *Phys. Rev. B: Condens. Matter Mater. Phys.* **2010**, *81*, 075405.
61. Kim, Y.; Hellmuth, T.; Bürkle, M.; Pauly, F.; Scheer, E. Characteristics of Amine-Ended and Thiol-Ended Alkane Single-Molecule Junctions Revealed by Inelastic Electron Tunneling Spectroscopy. *ACS Nano* **2011**, *5*, 4104–4111.
62. Barth, A. Infrared Spectroscopy of Proteins. *Biochim. Biophys. Acta, Bioenerg.* **2007**, *1767*, 1073–1101.
63. Kong, J.; Yu, S. Fourier Transform Infrared Spectroscopic Analysis of Protein Secondary Structures. *Acta Biochim. Biophys. Sin.* **2007**, *39*, 549–559.
64. Surewicz, W. K.; Szabo, A. G.; Mantsch, H. H. A Conformational Properties of Azurin in Solution as Determined from Resolution-enhanced Fourier-transform Infrared Spectra. *Eur. J. Biochem.* **1987**, *167*, 519–523.
65. Sepunaru, L.; Refaely-Abramson, S.; Lovrinčcić, R.; Gavrilov, Y.; Agrawal, P.; Levy, Y.; Kronik, L.; Pecht, I.; Sheves, M.; Cahen, D. Electronic Transport via Homopeptides: The Role of Side Chains and Secondary Structure. *J. Am. Chem. Soc.* **2015**, *137*, 9617–9626.
66. Venyaminov, S. Yu; Prendergast, F. G. Water (H_2O and D_2O) Molar Absorptivity in the 1000−4000 Cm-1 Range and Quantitative Infrared Spectroscopy of Aqueous Solutions. *Anal. Biochem.* **1997**, *248*, 234–45.
67. Paulsson, M.; Frederiksen, T.; Ueba, H.; Lorente, N.; Brandbyge, M. Unified Description of Inelastic Propensity Rules for Electron Transport through Nanoscale Junctions. *Phys. Rev. Lett.* **2008**, *100*, 226604.
68. Noy, G. Opto-electronic spectroscopy of molecular junctions. Ph.D. thesis, Tel Aviv University, Tel Aviv, Israel, 2011.
69. Yu, L.; Zangmeister, C.; Kushmerick, J. Origin of Discrepancies in Inelastic Electron Tunneling Spectra of Molecular Junctions. *Phys. Rev. Lett.* **2007**, *98*, 206803.
70. Ballistic transport is an established temperature-independent transport mechanism, but is extremely unlikely in a relatively disordered medium, like the one we are dealing with here. The idea of junctions with a very small, but nonzero activation barrier for hopping, or where tunneling and hopping occur simultaneously, has been suggested, theoretically, in ref 71. As our measurements go down to 10 K, where $kT \approx 0.9$ meV, this puts an upper barrier on the "very small" activation energy for transport. A so-called two-step tunneling mechanism, where a complete temperature

independence of the reorganization energy is assumed, was used in ref 72 to model our *I*−*V*−*T* Az data.
71. Hsu, L.-Y.; Wu, N.; Rabitz, H. Gate Control of the Conduction Mechanism Transition from Tunneling to Thermally Activated Hopping. *J. Phys. Chem. Lett.* **2014**, *5*, 1831–1836.
72. Valianti, S. Modeling the I-V characteristics in metal (semiconductor)−electron transfer protein−metal heterojunctions, MSc. Thesis, 2015, University of Cyprus.
73. Davis, J.; Wang, N.; Morgan, A.; Zhang, T.; Zhao, J. Metalloprotein Tunnel Junctions: Compressional Modulation of Barrier Height and Transport Mechanism. *Faraday Discuss.* **2006**, *131*, 167–179.
74. Thamann, T. J.; Frank, P.; Willis, L. J.; Loehr, T. M. Normal Coordinate Analysis of the Copper Center of Azurin and the Assignment of Its Resonance Raman Spectrum. *Proc. Natl. Acad. Sci. U. S. A.* **1982**, *79*, 6396–6400.
75. Woodruff, W. H.; Norton, K. A.; Swanson, B. I.; Fry, H. A. Temperature Dependence of the Resonance Raman Spectra of Plastocyanin and Azurin between Cryogenic and Ambient Conditions. *Proc. Natl. Acad. Sci. U. S. A.* **1984**, *81*, 1263–1267.
76. Baldacchini, C.; Bizzarri, A.; Cannistraro, S. Excitation of the Ligand-to-Metal Charge Transfer Band Induces Electron Tunnelling in Azurin. *Appl. Phys. Lett.* **2014**, *104*, 093702.
77. Book, L. D.; Arnett, D. C.; Hu, H.; Scherer, N. F. Ultrafast Pump-Probe Studies of Excited-State Charge-Transfer Dynamics in Blue Copper Proteins. *J. Phys. Chem. A* **1998**, *102*, 4350–4359.
78. Artés, J.; López-Martínez, M.; Giraudet, A.; Díez-Pérez, I.; Sanz, F.; Gorostiza, P. Current-Voltage Characteristics and Transition Voltage Spectroscopy of Individual Redox Proteins. *J. Am. Chem. Soc.* **2012**, *134*, 20218–20221.
79. Artés, J.; López-Martínez, M.; Díez-Pérez, I.; Sanz, F.; Gorostiza, P. Conductance Switching in Single Wired Redox Proteins. *Small* **2014**, *10*, 2537–2541.
80. Amdursky, N.; Ferber, D.; Pecht, I.; Sheves, M.; Cahen, D. Redox Activity Distinguishes Solid-State Electron Transport from Solution-Based Electron Transfer in a Natural and Artificial Protein: Cytochrome C and Hemin-Doped Human Serum Albumin. *Phys. Chem. Chem. Phys.* **2013**, *15*, 17142–17149.
81. Migliore, A.; Nitzan, A. Irreversibility and Hysteresis in Redox Molecular Conduction Junctions. *J. Am. Chem. Soc.* **2013**, *135*, 9420–9432.
82. Arielly, R.; Vadai, M.; Kardash, D.; Noy, G.; Selzer, Y. Real-Time Detection of Redox Events in Molecular Junctions. *J. Am. Chem. Soc.* **2014**, *136*, 2674–2680.
83. Fleming, B. D.; Praporski, S.; Bond, A. M.; Martin, L. L. Electrochemical Quartz Crystal Microbalance Study of Azurin Adsorption onto an Alkanethiol Self-Assembled Monolayer on Gold. *Langmuir* **2008**, *24*, 323–327.